Supporting Information

Design of "turn-off" luminescent Ln-MOFs for sensitive detection of cyanide anion

Weisai Liu,[a,b,c] Fei Wang,*[a,b,c] Xiaoyi Chen,[c] Wenke Zhi,[c] Xuquan Wang,[c] Baoqiang Xu[a] and Bin Yang[a]

a. National Engineering Research Center of Vacuum Metallurgy, Kunming 650093, China.

b. Key Laboratory of Vacuum Metallurgy for Nonferrous Metal of Yunnan Province, Kunming 650093, China

c. Faculty of Metallurgical and Energy Engineering, Kunming University of Science and Technology, Kunming 650093, China.

Corresponding author: Fei Wang, E-mail: feiwang@kust.edu.cn;

Crystallographic Data Collection and Structure Determination

Single-crystal X-ray diffraction data of Ln-MOFs **1** and **2** were collected at 150(10) K using a Rigaku HyPix diffractometer with graphite-monochromatic Mo Kα radiation (λ = 0.71073 Å). An empirical absorption correction was applied using the SADABS program. The program Olex2 was used to solve the structures of Ln-MOFs **1** and **2**. All the structures were solved with ShelXT using intrinsic phasing and refined with full-matrix least-squares method on F^2 by using the ShelXL refinement package. All non-hydrogen atoms were refined and treated anisotropically. The diffraction contribution of disordered solvent molecules in the structure were removed by the PLATON/SQUEEZE. The Ln-MOFs **1** and **2** topological type was explored from the crystallographic data with TOPOS Pro software.

Table S1. Crystallographic data and structure refinement for **1** and **2**

Compound	**1**	**2**
CCDC number	2106266	2106267
Formula	$C_{21}H_{24}Br_3EuN_3O_9$	$C_{21}H_{24}Br_3N_3O_9Tb$
$D_{calc.}$/ g cm^{-3}	2.057	2.091
μ/mm^{-1}	6.673	7.011
Formula Weight	854.12	861.08
Size/mm^3	0.12×0.11×0.10	0.12 × 0.11 × 0.10
T/K	149.98(10)	150.04(10)
Crystal System	triclinic	triclinic
Space Group	P-1	P-1
a/Å	11.2941(2)	11.2415(3)
b/Å	11.5981(2)	11.5520(3)
c/Å	12.9541(3)	12.9279(4)
α/°	108.813(2)	109.079(3)
β/°	114.558(2)	114.551(3)
γ/°	98.648(2)	97.782(2)
V/Å^3	1378.90(5)	1369.46(8)
Z	2	2
Wavelength/Å	0.71073	0.71073
Radiation type	Mo Kα	Mo Kα
Θ_{min}/°	1.912	1.913
Θ_{max}/°	29.481	29.482
Measured Refl's.	30072	31328
Refl's I≥2σ(I)	5641	5384
Indep't Refl's	6452	6425
R_{int}	0.0364	0.0588
Parameters	388	388
Restraints	240	120
GooF	1.051	1.065
Final R indexes [I>=2σ (I)]	R_1=0.0233 wR_2=0.0464	R_1=0.0414 wR_2=0.1041
Final R indexes [all data]	R_1=0.0303 wR_2=0.0481	R_1=0.0530 wR_2=0.1094

Table S2. Selected Bond Lengths (Å) and Angles (°) for **1**.

Eu1-O1	2.3645(17)	N2-C16	1.320(4)
Eu1-O1^{i}	2.6528(17)	N2-C17	1.462(5)
Eu1-O2^{i}	2.5144(19)	N2-C18	1.447(5)
Eu1-O3^{ii}	2.4555(19)	C1-C2	1.385(4)
Eu1-O4^{ii}	2.4925(19)	C1-C6	1.394(4)
Eu1-O5	2.3781(17)	C1-C7	1.501(4)
Eu1-O6^{i}	2.4161(18)	C2-C3	1.372(4)
Eu1-O7	2.4238(17)	C3-C4	1.401(4)
Eu1-O8	2.4417(19)	C4-C5	1.399(4)
Br1-C2	1.904(3)	C4-C8	1.510(4)
Br2-C5	1.900(3)	C5-C6	1.384(4)
Br3-C10	1.902(3)	C9-C10	1.388(3)
O1-C7	1.259(3)	C9-C11^{iii}	1.394(4)
O2-C7	1.248(3)	C9-C12	1.513(3)
O3-C8	1.257(3)	C10-C11	1.384(4)
O4-C8	1.255(3)	O9-C19	1.177(7)
O5-C12	1.258(3)	N3-C19	1.351(7)
O6-C12	1.257(3)	N3-C20	1.458(7)
O7-C13	1.229(3)	N3-C21	1.452(7)
O8-C16	1.236(3)	N3A-C19A	1.381(8)
N1-C13	1.325(4)	N3A-C20A	1.469(8)
N1-C14	1.443(5)	N3A-C21A	1.435(8)
N1-C15	1.440(5)	O9A-C19A	1.191(8)
O1-Eu1-O1^{i}	71.05(6)	C16-N2-C17	120.8(3)
O1-Eu1-O2^{i}	121.13(6)	C16-N2-C18	121.0(3)
O1-Eu1-O3^{ii}	84.46(6)	C18-N2-C17	118.1(3)
O1-Eu1-O4^{ii}	75.86(6)	C2-C1-C6	117.7(2)
O1-Eu1-O5	74.85(6)	C2-C1-C7	123.0(2)
O1-Eu1-O6^{i}	75.14(6)	C6-C1-C7	119.3(2)
O1-Eu1-O7	144.58(6)	C1-C2-Br1	119.6(2)
O1-Eu1-O8	140.49(6)	C3-C2-Br1	118.8(2)
O2^{i}-Eu1-O1^{i}	50.09(5)	C3-C2-C1	121.6(2)
O3^{ii}-Eu1-O1^{i}	148.65(6)	C2-C3-C4	121.2(2)
O3^{ii}-Eu1-O2^{i}	147.99(6)	C3-C4-C8	116.1(2)
O3^{ii}-Eu1-O4^{ii}	52.55(6)	C5-C4-C3	117.3(2)
O4^{ii}-Eu1-O1^{i}	133.71(6)	C5-C4-C8	126.6(2)
O4^{ii}-Eu1-O2^{i}	145.93(6)	C4-C5-Br2	124.1(2)
O5-Eu1-O1^{i}	67.29(6)	C6-C5-Br2	115.0(2)
O5-Eu1-O2^{i}	82.60(6)	C6-C5-C4	120.9(2)

O5-Eu1-O3^{ii}	125.52(6)	C5-C6-C1	121.2(2)
O5-Eu1-O4^{ii}	73.49(6)	O1-C7-Eu1^{i}	64.09(13)
O5-Eu1-O6^{i}	133.16(6)	O1-C7-C1	118.5(2)
O5-Eu1-O7	140.50(6)	O2-C7-Eu1^{i}	57.71(13)
O5-Eu1-O8	73.05(6)	O2-C7-O1	121.8(2)
O6^{i}-Eu1-O1^{i}	69.36(6)	O2-C7-C1	119.7(2)
O6^{i}-Eu1-O2^{i}	83.13(6)	C1-C7-Eu1^{i}	177.36(17)
O6^{i}-Eu1-O3^{ii}	85.95(6)	O3-C8-Eu1^{ii}	59.84(13)
O6^{i}-Eu1-O4^{ii}	130.94(6)	O3-C8-C4	118.4(2)
O6^{i}-Eu1-O7	75.07(6)	O4-C8-Eu1^{ii}	61.52(14)
O6^{i}-Eu1-O8	144.37(6)	O4-C8-O3	121.4(2)
O7-Eu1-O1^{i}	114.83(6)	O4-C8-C4	120.2(2)
O7-Eu1-O2^{i}	73.37(6)	C4-C8-Eu1^{ii}	178.18(18)
O7-Eu1-O3^{ii}	74.76(6)	C10-C9-C11^{iii}	117.9(2)
O7-Eu1-O4^{ii}	110.97(6)	C10-C9-C12	124.5(2)
O7-Eu1-O8	71.20(6)	C11^{iii}-C9-C12	117.6(2)
O8-Eu1-O1^{i}	115.46(6)	C9-C10-Br3	120.22(19)
O8-Eu1-O2^{i}	76.65(7)	C11-C10-Br3	118.05(19)
O8-Eu1-O3^{ii}	95.87(7)	C11-C10-C9	121.7(2)
O8-Eu1-O4^{ii}	73.40(7)	C10-C11-C9^{iii}	120.5(2)
Eu1-O1-Eu1^{i}	108.95(6)	O5-C12-C9	114.5(2)
C7-O1-Eu1^{i}	90.64(15)	O6-C12-O5	127.3(2)
C7-O1-Eu1	160.36(17)	O6-C12-C9	118.2(2)
C7-O2-Eu1^{i}	97.48(15)	O7-C13-N1	124.8(3)
C8-O3-Eu1^{ii}	93.88(15)	O8-C16-N2	124.9(3)
C8-O4-Eu1^{ii}	92.21(16)	C19-N3-C20	118.9(7)
C12-O5-Eu1	138.50(16)	C19-N3-C21	121.4(6)
C12-O6-Eu1^{i}	135.86(15)	C21-N3-C20	119.5(6)
C13-O7-Eu1	125.31(18)	O9-C19-N3	123.5(7)
C16-O8-Eu1	123.83(18)	C19A-N3A-C20A	120.7(8)
C13-N1-C14	121.2(3)	C19A-N3A-C21A	119.7(8)
C13-N1-C15	121.6(3)	C21A-N3A-C20A	119.5(8)
C15-N1-C14	117.1(3)	O9A-C19A-N3A	124.4(8)

Symmetry codes: (i) 1-X, -Y, 1-Z; (ii) 1-X, 1-Y, 1-Z; (iii) -X, -Y, 1-Z

Table S3. Selected Bond Lengths (Å) and Angles (˚) for 2

Tb1-O1	2.335(3)	N2-C16	1.313(7)
Tb1-O1^{i}	2.650(3)	N2-C17	1.440(7)
Tb1-O2^{i}	2.483(3)	N2-C18	1.455(7)
Tb1-O3^{ii}	2.475(3)	C1-C2	1.385(6)
Tb1-O4^{ii}	2.434(3)	C1-C6	1.383(6)
Tb1-O5	2.350(3)	C1-C7	1.509(6)
Tb1-O6^{i}	2.387(3)	C2-C3	1.390(6)
Tb1-O7	2.421(3)	C3-C4	1.391(6)
Tb1-O8	2.397(3)	C4-C5	1.405(6)
Br1-C2	1.895(5)	C4-C8	1.507(6)
Br2-C5	1.901(5)	C5-C6	1.386(6)
Br3-C12	1.902(4)	C9-C10	1.525(6)
O1-C7	1.255(6)	C10-C11	1.390(6)
O2-C7	1.245(6)	C10-C12^{iii}	1.391(6)
O3-C8	1.254(6)	C11-C12	1.382(6)
O4-C8	1.261(6)	O9-C19	1.175(18)
O5-C9	1.251(6)	N3-C19	1.35(2)
O6-C9	1.261(6)	N3-C20	1.42(2)
O7-C13	1.241(6)	N3-C21	1.422(19)
O8-C16	1.227(6)	O9A-C19A	1.194(17)
N1-C13	1.316(7)	C19A-N3A	1.35(2)
N1-C14	1.459(8)	N3A-C20A	1.458(18)
N1-C15	1.448(8)	N3A-C21A	1.43(3)
O1-Tb1-O1^{i}	71.01(11)	C16-N2-C17	121.1(6)
O1-Tb1-O2^{i}	121.43(11)	C16-N2-C18	121.6(5)
O1-Tb1-O3^{ii}	75.74(11)	C17-N2-C18	117.2(5)
O1-Tb1-O4^{ii}	84.06(12)	C2-C1-C7	122.0(4)
O1-Tb1-O5	75.18(11)	C6-C1-C2	118.8(4)
O1-Tb1-O6^{i}	75.17(11)	C6-C1-C7	119.2(4)
O1-Tb1-O7	140.86(11)	C1-C2-Br1	120.6(3)
O1-Tb1-O8	144.23(11)	C1-C2-C3	120.4(4)
O2^{i}-Tb1-O1^{i}	50.42(10)	C3-C2-Br1	119.0(3)
O3^{ii}-Tb1-O1^{i}	133.70(11)	C2-C3-C4	121.7(4)
O3^{ii}-Tb1-O2^{i}	145.82(11)	C3-C4-C5	117.1(4)
O4^{ii}-Tb1-O1^{i}	147.82(12)	C3-C4-C8	116.3(4)
O4^{ii}-Tb1-O2^{i}	147.79(11)	C5-C4-C8	126.6(4)
O4^{ii}-Tb1-O3^{ii}	53.08(11)	C4-C5-Br2	123.8(3)
O5-Tb1-O1^{i}	67.14(10)	C6-C5-Br2	115.3(3)
O5-Tb1-O2^{i}	82.13(11)	C6-C5-C4	121.0(4)

O5-Tb1-O3^{ii}	73.91(11)	C1-C6-C5	121.0(4)
O5-Tb1-O4^{ii}	126.41(11)	O1-C7-Tb1^{i}	65.1(2)
O5-Tb1-O6^{i}	133.28(11)	O1-C7-C1	118.1(4)
O5-Tb1-O7	73.33(11)	O2-C7-Tb1^{i}	57.4(2)
O5-Tb1-O8	140.51(12)	O2-C7-O1	122.5(4)
O6^{i}-Tb1-O1^{i}	69.46(10)	O2-C7-C1	119.4(4)
O6^{i}-Tb1-O2^{i}	83.49(11)	C1-C7-Tb1^{i}	176.8(3)
O6^{i}-Tb1-O3^{ii}	130.69(11)	O3-C8-Tb1^{ii}	61.6(2)
O6^{i}-Tb1-O4^{ii}	84.99(11)	O3-C8-O4	121.4(4)
O6^{i}-Tb1-O7	143.96(12)	O3-C8-C4	120.3(4)
O6^{i}-Tb1-O8	74.73(11)	O4-C8-Tb1^{ii}	59.8(2)
O7-Tb1-O1^{i}	115.79(11)	O4-C8-C4	118.3(4)
O7-Tb1-O2^{i}	76.34(12)	C4-C8-Tb1^{ii}	178.0(3)
O7-Tb1-O3^{ii}	73.67(12)	O5-C9-O6	128.0(4)
O7-Tb1-O4^{ii}	96.39(12)	O5-C9-C10	114.8(4)
O8-Tb1-O1^{i}	114.90(10)	O6-C9-C10	117.1(4)
O8-Tb1-O2^{i}	73.46(11)	C11-C10-C9	117.3(4)
O8-Tb1-O3^{ii}	110.98(12)	C11-C10-C12^{iii}	118.3(4)
O8-Tb1-O4^{ii}	74.51(12)	C12^{iii}-C10-C9	124.3(4)
O8-Tb1-O7	71.06(12)	C12-C11-C10	120.1(4)
Tb1-O1-Tb1^{i}	108.99(11)	C10^{iii}-C12-Br3	120.1(3)
C7-O1-Tb1	161.5(3)	C11-C12-Br3	118.3(3)
C7-O1-Tb1^{i}	89.5(3)	C11-C12-C10^{iii}	121.6(4)
C7-O2-Tb1^{i}	97.6(3)	O7-C13-N1	124.5(5)
C8-O3-Tb1^{ii}	91.9(3)	O8-C16-N2	125.8(5)
C8-O4-Tb1^{ii}	93.6(3)	C19-N3-C20	121.3(15)
C9-O5-Tb1	138.4(3)	C19-N3-C21	120.7(16)
C9-O6-Tb1^{i}	135.3(3)	C20-N3-C21	117.8(15)
C13-O7-Tb1	123.7(3)	O9-C19-N3	124.5(18)
C16-O8-Tb1	126.1(3)	O9A-C19A-N3A	126.7(16)
C13N1-C14	120.7(6)	C19A-N3A-C20A	122.0(14)
C13-N1-C15	120.8(5)	C19A-N3A-C21A	121.1(16)
C15-N1-C14	118.5(5)	C21A-N3A-C20A	116.8(16)

Symmetry codes: (i) 1-X, -Y, 1-Z; (ii) 1-X, 1-Y, 1-Z; (iii) -X, -Y, 1-Z

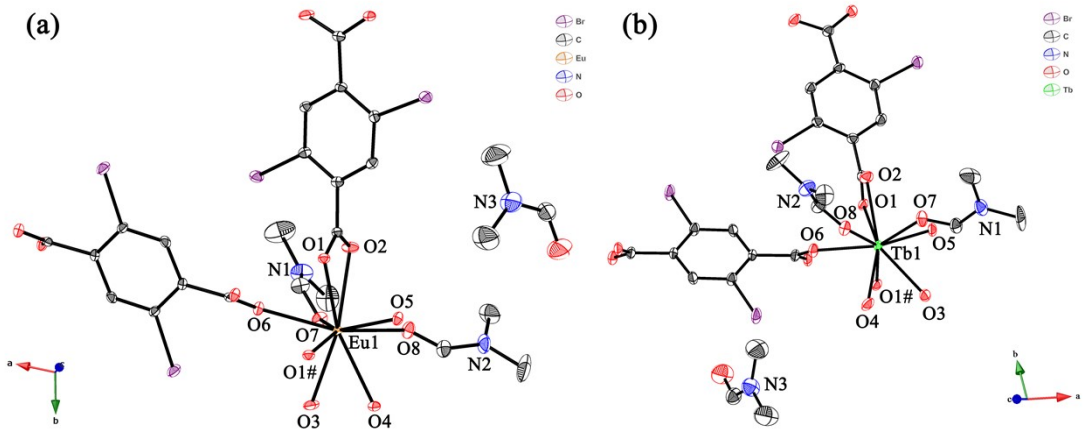

Fig. S1 ORTEP diagrams of the structural unit **1** and **2** with partial atom numbering schemes, the thermal displacement ellipsoids are drawn at 40% probability. Hydrogen atoms have been omitted for clarity.

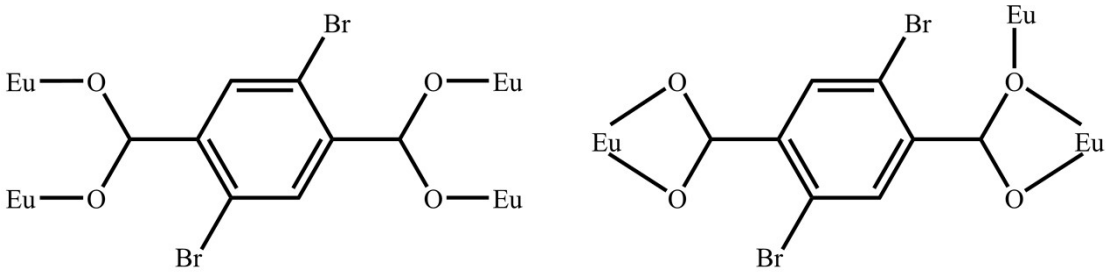

$(k^1\text{-}k^1)\text{-}(k^1\text{-}k^1)\text{-}\mu_4\text{-DBTA}^{2-}$ **$(k^2)\text{-}(k^1\text{-}k^2\text{-}\mu_2)\text{-}\mu_3\text{-DBTA}^{2-}$**

Fig. S2 The coordination modes of $DBTA^{2-}$ ligand.

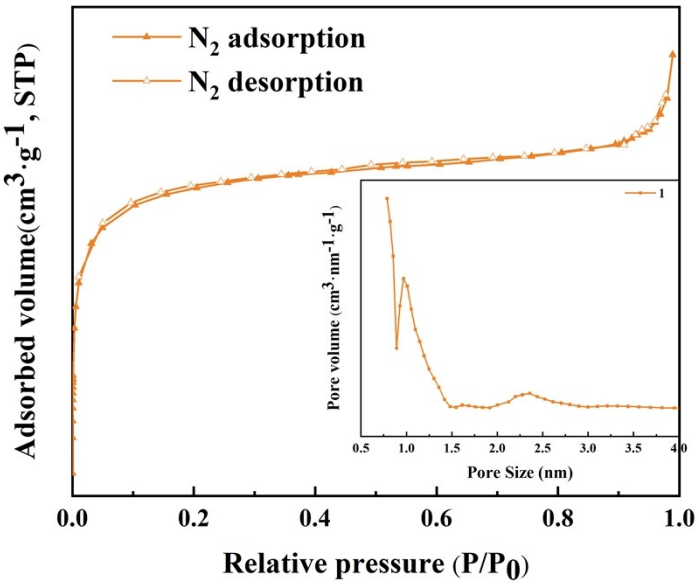

Fig. S3 N_2 adsorption-desorption isotherms of **1**, insert: Pore size distribution plot.

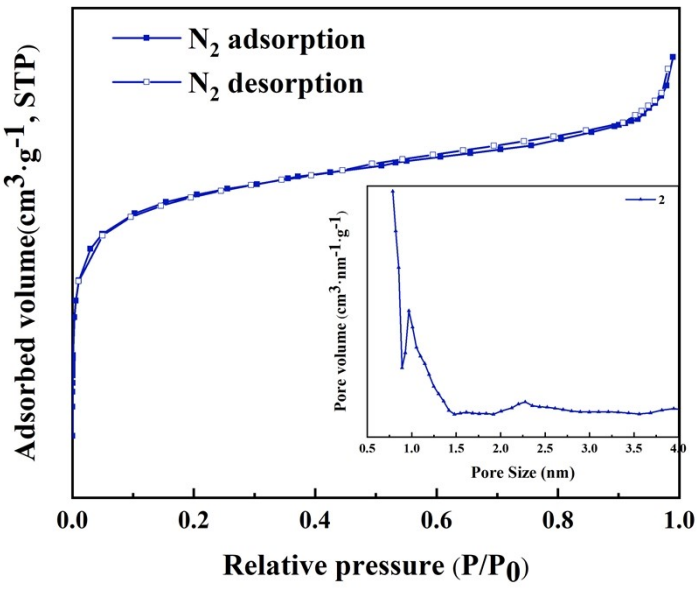

Fig. S4 N_2 adsorption-desorption isotherms of **2**, insert: Pore size distribution plot.

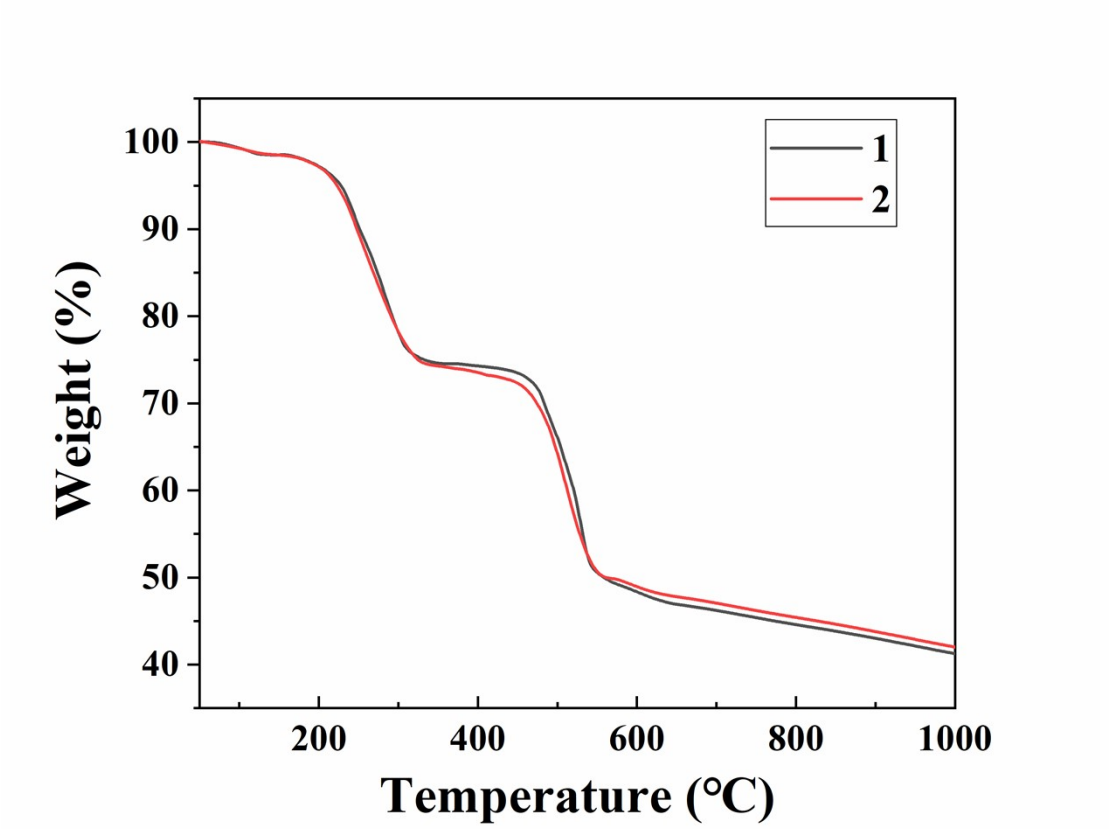

Fig. S5 Thermogravimetric curve of **1** and **2**.

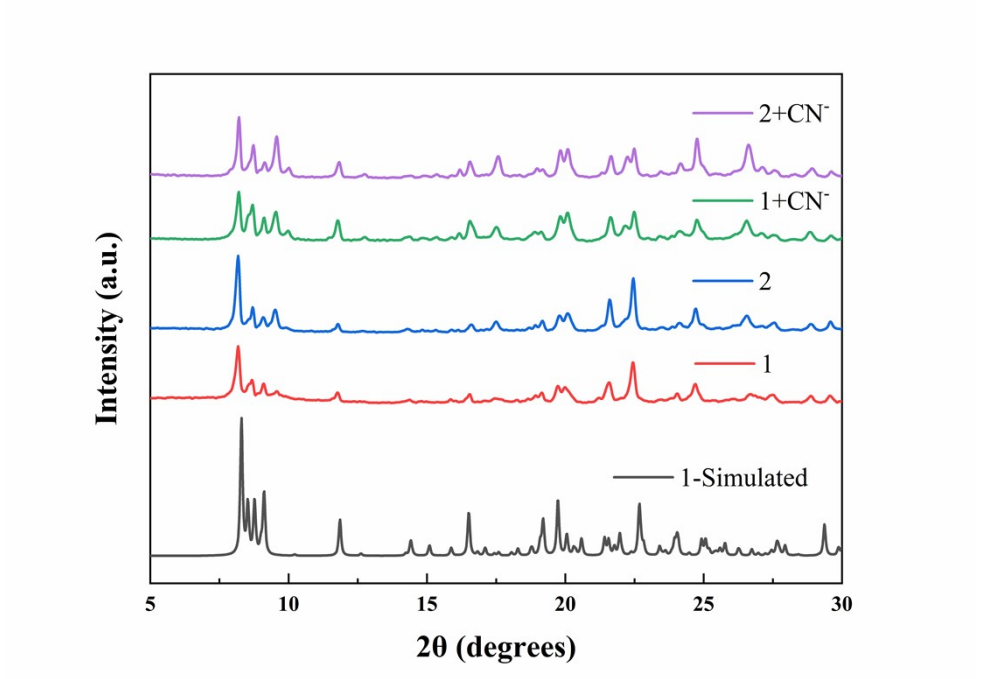

Fig. S6 Simulated PXRD patterns of **1** and synthesized PXRD of compounds **1**, **2**, **1**+CN^- and **2**+CN^-.

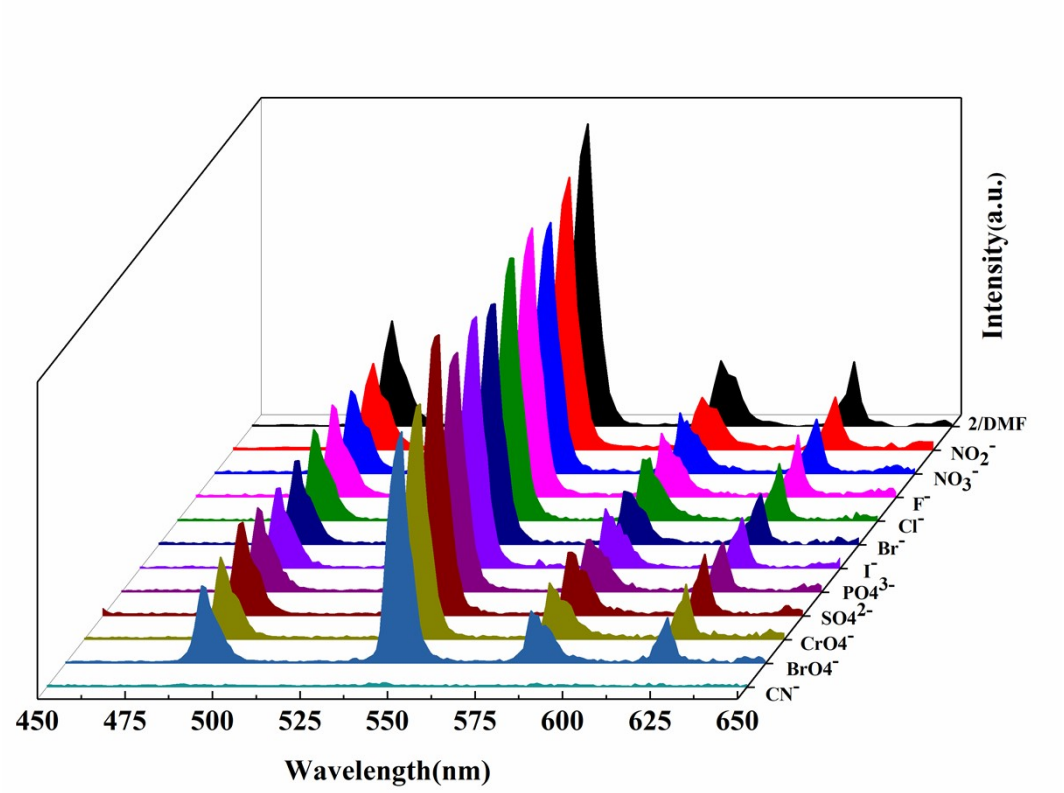

Fig. S7 Emission spectra and luminescence intensity at 546 nm of **2**/DMF treated with different anions (λex=303 nm, 100 μg/mL).

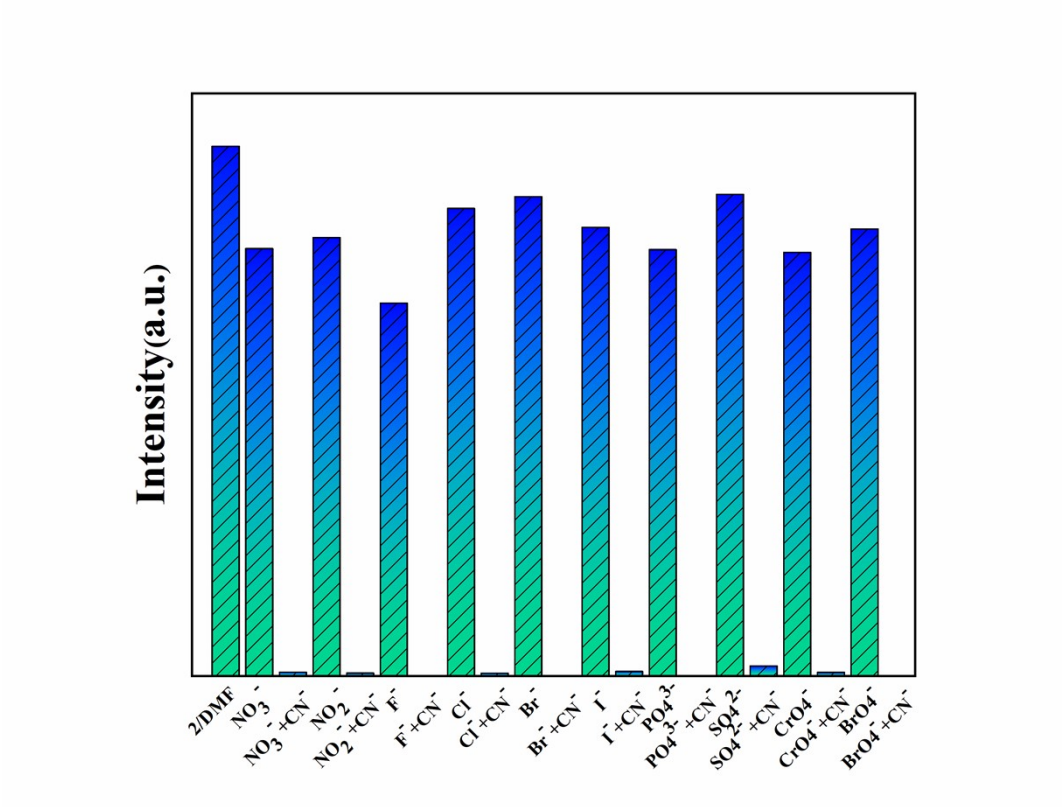

Fig. S8 Comparison of the luminescence intensity (546 nm) of **2**/DMF suspension dispersion mixed with interfering anions (λex=303 nm, 100 μg/mL)

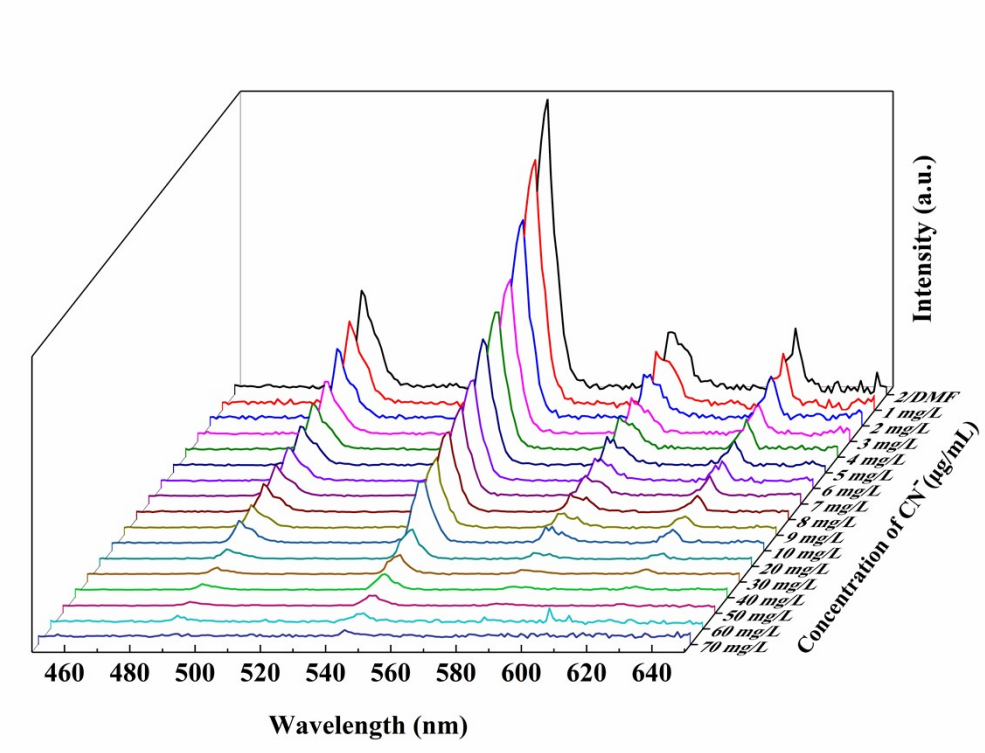

Fig. S9 Emission spectra of **2**/DMF with different concentrations of CN^-(1-70 μg/mL)

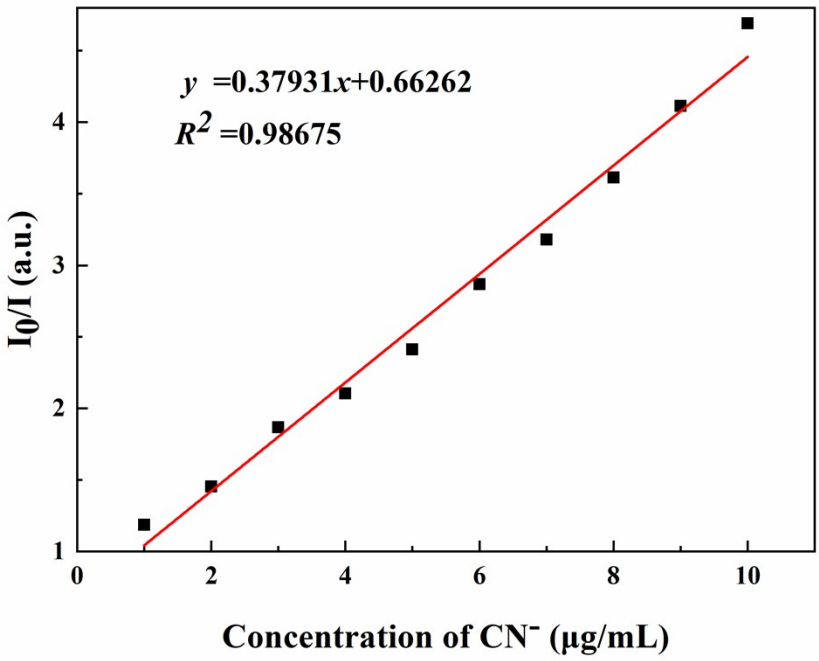

Fig. S10 Relationship between I_0/I and different CN^- concentrations and Stern-Volmer formula fitting of **2** with concentrations of 1-10 μg/mL.

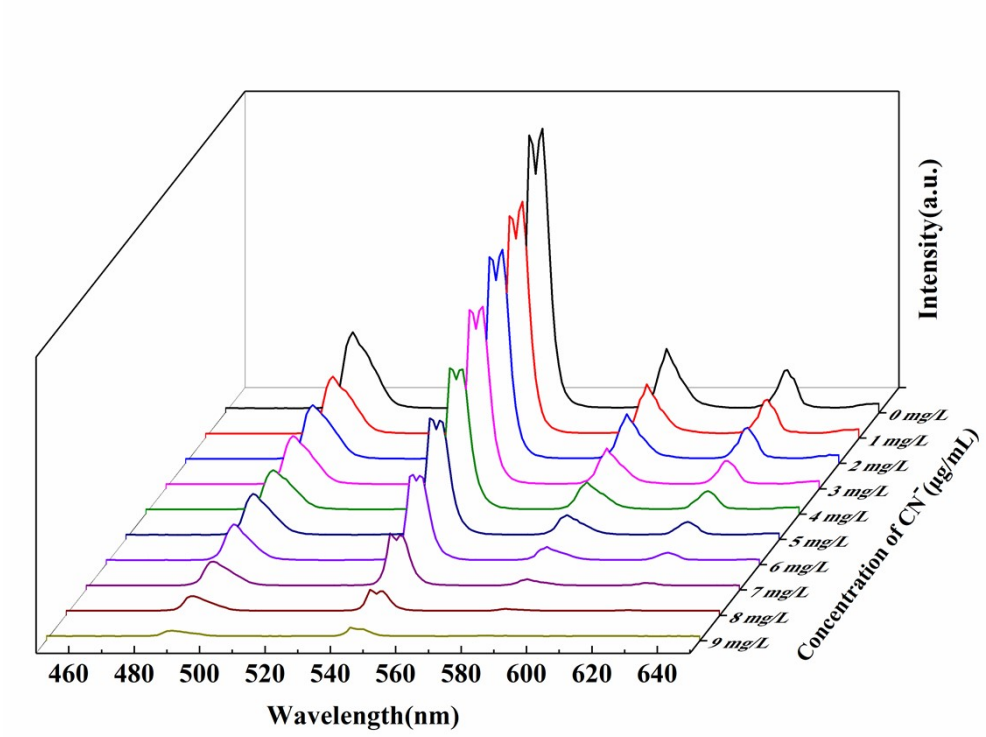

Fig. S11 Emission spectra of **2** with different concentrations of CN^-(1-9 μg/mL) in aqueous solution.

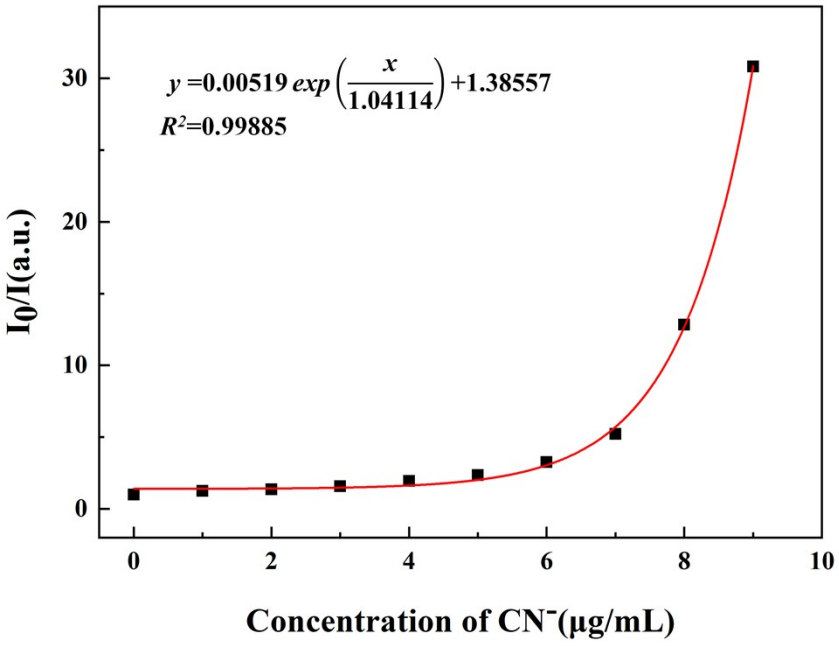

Fig. S12 Relationship between I_0/I and different CN^- concentrations of **2**.

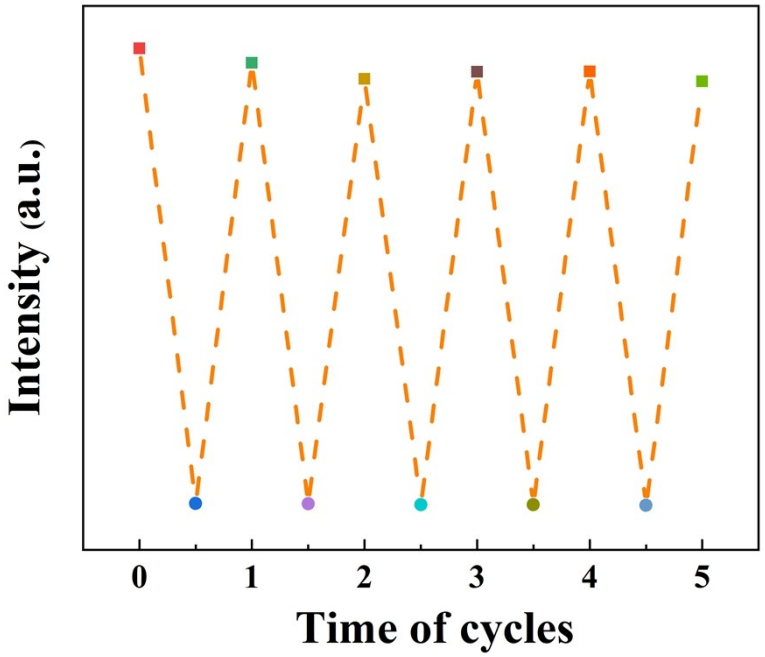

Fig. S13 Fluorescence intensity (619 nm) of **1** during five recycles.

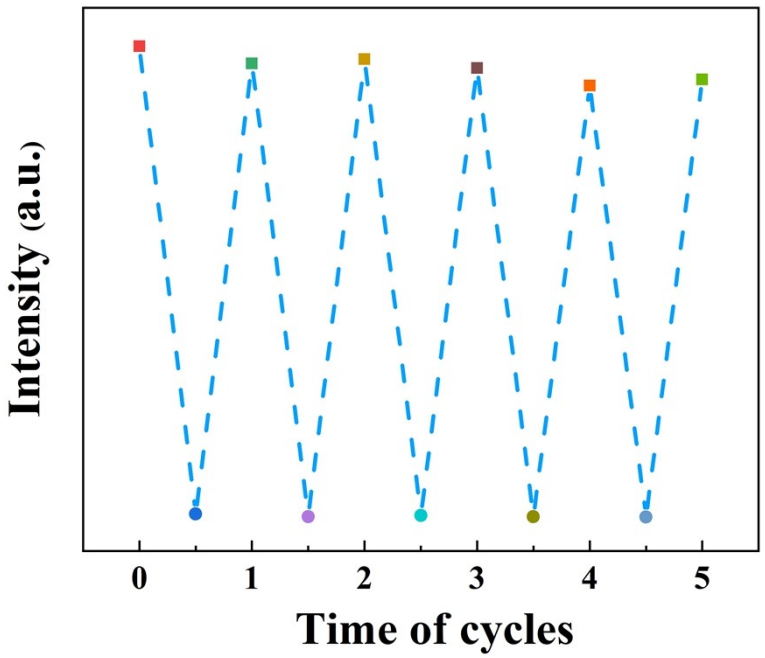

Fig. S14 Fluorescence intensity (546 nm) of **2** during five recycles.

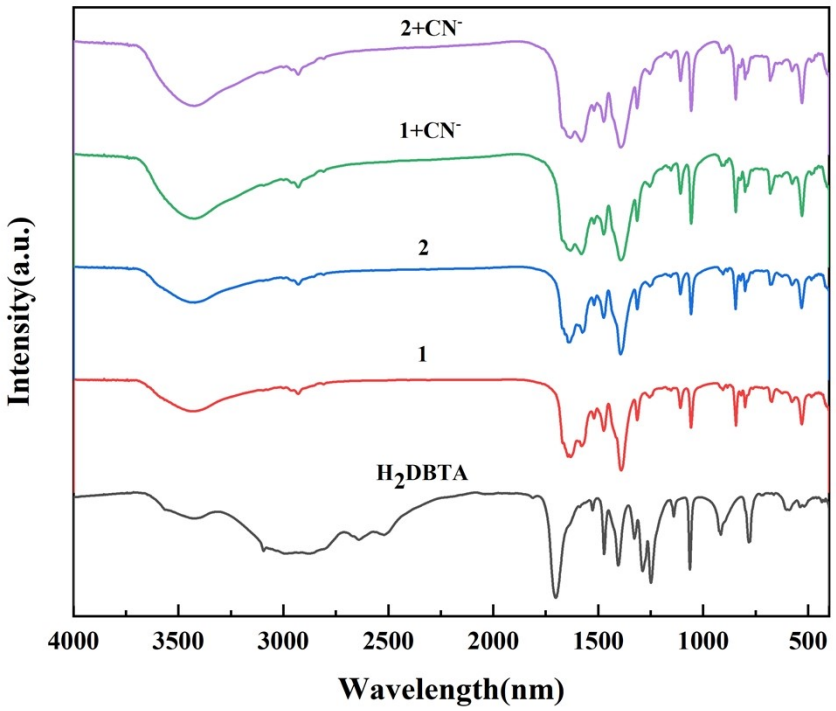

Fig. S15 FT-IR spectra of ligand, **1**, **2**, **1**+CN^- and **2**+CN^-.

Table S4. Comparison of the LOD values of CN^- with other materials.

Material	Solvent	LOD	Ref.
1	DMF	1.691 μM	This work
2	DMF	8.307 μM	This work
2-HPEAPB	CH_3CN-H_2O	8.0 μM	1
$[Hf_6O_4(OH)_4(C_8H_2O_4S_2)_6]\cdot 9H_2O\cdot 2DMF$	H_2O	0.35 μM	2
4-(p-tolyl)thiazol-2-amine and 2-hydroxy-1-naphthaldehyde	Bis-tris buffer/DMSO	19.4 μM	3
6,7-dihydroxycoumarin	DMSO-water	5.77 μM	4
HBTM-HC	DMSO	1.38 μM	5
triarylborane substituted bisthiazole	THF	2.1 μM	6
L	DMSO/H_2O	6.4 μM	7
M-ZIF-90	H_2O/DMSO	2 μM	8
bio-MOF-1⊃DAAC	H_2O	5.2 ppb	9
TIP-Co	THF-H_2O	89.3 nM	10
$CuCl_2$@MOF-867	H_2O	0.19 μM	11

References

1. X. X. Ou, Y. L. Jin, X. Q. Chen, C. B. Gong, X. B. Ma, Y. S. Wang, C. F. Chow and Q. Tang, *Anal. Methods*, 2015, **7**, 5239-5244.
2. R. Dalapati, S. Nandi and S. Biswas, *Dalton Trans.*, 2020, **49**, 8684-8692.
3. S. M. Kim, M. Kang, I. Choi, J. J. Lee and C. Kim, *New J. Chem.*, 2016, **40**, 7768-7778.
4. R. Kaushik, A. Ghosh, A. Singh, P. Gupta, A. Mittal and D. A. Jose, *Acs Sensors*, 2016, **1**, 1265-1271.
5. L. Tang, L. Zhou, A. Liu, X. Yan, K. Zhong, X. Liu, X. Gao and J. Li, *Dyes Pigm.*, 2021, **186**, 109034.
6. R. Maragani, T. S. Reddy and R. Misra, *Tetrahedron Lett.*, 2016, **57**, 3853-3857.
7. Z. Li, C. Liu, S. Wang, L. Xiao and X. Jing, *Spectrochim. Acta, Part A*, 2019, **210**, 321-328.
8. A. Karmakar, N. Kumar, P. Samanta, A. V. Desai and S. K. Ghosh, *Chem. - Eur. J.*, 2016, **22**, 864-868.
9. A. Karmakar, B. Joarder, A. Mallick, P. Samanta, A. V. Desai, S. Basu and S. K. Ghosh, *Chem. Commun.*, 2017, **53**, 1253-1256.
10. Y. Liu, Q. Qiu, X. Zhang, K. Huang and D. Qin, *J. Solid State Chem.*, 2021, **300**, 122258.
11. D. Mahato, S. Fajal, P. Samanta, W. Mandal and S. K. Ghosh, *ChemPlusChem*, 2022, **87**, e202100426.